

Exploring the Protective and Reparative Mechanisms of *G. lucidum* Polysaccharides Against H₂O₂-Induced Oxidative Stress in Human Skin Fibroblasts

Xiuqin Shi^{1,2}
Wenjing Cheng^{1,3,4}
Qian Wang¹
Jiachan Zhang^{1,3,4}
Changtao Wang^{1,3,4}
Meng Li^{1,3,4}
Dan Zhao^{1,3,4}
Dongdong Wang^{1,3,4}
Quan An²

¹Chemistry and Materials Engineering, Beijing Technology and Business University, Beijing, 100048, People's Republic of China; ²Yunnan Baiyao Group Co., Ltd, Kunming, 650000, People's Republic of China; ³Beijing Key Lab of Plant Resource Research and Development, Beijing Technology and Business University, Beijing, 100048, People's Republic of China; ⁴Institute of Cosmetic Regulatory Science, Beijing Technology and Business University, Beijing, 100048, People's Republic of China

Correspondence: Jiachan Zhang;
Changtao Wang
College of Chemistry and Materials
Engineering, Beijing Technology and
Business University, 11 Fucheng Road,
Haidian District, Beijing, 100048, People's
Republic of China
Tel +86-13426258535; +86-18910839617
Email xiaochan8787@163.com;
wangct@th.btbu.edu.cn

Background: *Ganoderma lucidum* (*G. lucidum*) is one of China's traditional medicinal materials. *G. lucidum* polysaccharide has a wide range of promising pharmacological applications. However, there are many kinds of *G. lucidum* and they contain different kinds of polysaccharides. The biological mechanism through which *Ganoderma lucidum* polysaccharides (GLP) is able to protect human skin fibroblasts (HSFs) from H₂O₂-induced oxidative damage is still unclear.

Methods: Six polysaccharides were obtained from *G. lucidum* to evaluate their free radical scavenging ability (DPPH free radical, ABTS free radical, hydroxyl-free radical, superoxide anion-free radical) in vitro, and their protective and reparative effects on oxidative damage induced by H₂O₂ in human skin fibroblasts. One polysaccharide was selected to detect oxidative damage markers and gene expression in the Keap1-Nrf2/ARE signaling pathway in HSFs.

Results: All six polysaccharides showed the ability to scavenge free radicals and enhance the tolerance of human skin fibroblasts to H₂O₂ damage. Among them, GLP1 was selected and separated into two components (GLP1I and GLP1II). The results showed that GLP1, GLP1I and GLP1II could significantly reduce the levels of reactive oxygen species (ROS) and malondialdehyde (MDA). The protective effect of GLP1II was stronger than that of positive control vitamin C. In addition, GLP1, GLP1I and GLP1II could significantly increase the levels of superoxide dismutase (SOD), catalase (CAT) and glutathione peroxidase (GSH-Px). And GLP1I works best in both ways. Meanwhile, Nrf2, a key regulator of Keap1-NRF2/ARE signaling pathway, was activated, while Keap1, a negative regulator, was inhibited, thus promoting the expression of downstream antioxidant enzyme genes (GSTs, GCLs, Nqo1, and Ho-1).

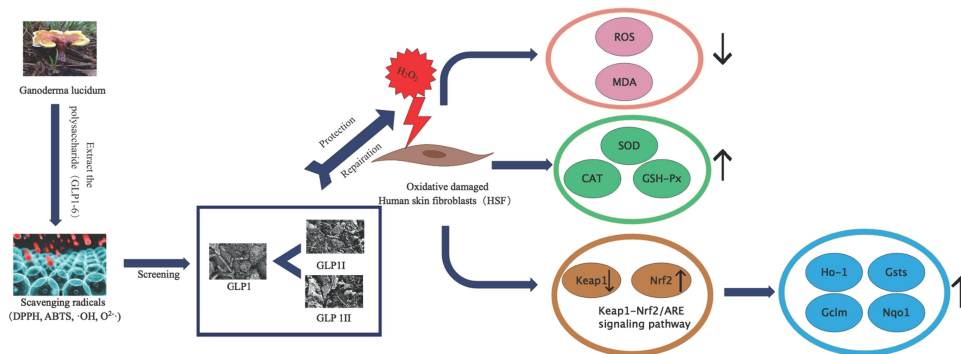
Conclusion: The results showed that GLP could protect human skin fibroblasts from oxidative damage caused by H₂O₂ peroxide by enhancing enzyme activity and activating Keap1-Nrf2/ARE signaling pathway. GLP will act as a natural antioxidant to protect the skin from oxidative stress damage.

Keywords: *Ganoderma lucidum*, polysaccharide, oxidative stress, Keap1-Nrf2/ARE signaling pathway

Introduction

Ganoderma lucidum (*G. lucidum*) is a traditional Chinese medicinal material with peculiar medicinal value.¹ The most attractive characteristic of *G. lucidum* is that it can regulate immunity and inhibit tumor activity.²⁻⁵ In recent years, in vivo and in vitro studies have shown that *G. lucidum* can lower blood glucose and has an

Graphical Abstract



anti-cancer, anti-oxidative, anti-inflammatory, and anti-aging effects.^{6–11} The main active ingredients of *G. lucidum* are *G. lucidum* polysaccharide (GLP), triterpene, and *G. lucidum* acid.¹² More than 200 kinds of polysaccharides have been isolated, most of which are β -glucan and a few are α -glucan. The polysaccharide chain is composed of three monosaccharide chains, which is a helical stereostructure, its stereostructure is similar to DNA and RNA, and the helical layers are mainly fixed by hydrogen bonds. Ganoderma polysaccharides are mostly heterosaccharides, that is, in addition to glucose, most of them also contain a small amount of arabinose, xylose, fucose, rhamnose, galactose and other monosaccharides. Triterpenoids of *G. lucidum* were mainly distributed in the outer part of the fruiting body, and the content increased with the maturity of the fruiting body. Some triterpenoids are bitter, some are not bitter, and the content of triterpenoids varies with varieties, culture conditions and different growth stages. Ganoderic acid is a triterpenoid substance. However, the main active pharmacodynamic component of *G. lucidum* is GLP, with a wide range of pharmacological activities.¹³ GLP has a complex structure and molecular weight ranging from 100 to 100,000 of kDa. Up to now, more than 200 different polysaccharides have been discovered.¹⁴ It has been found that GLP has an excellent performance in terms of antioxidant efficacy.^{15–18} As an effective antioxidant, GLP can effectively reduce oxidative damage by scavenging DPPH-, O-, and OH-free radicals and enhancing the antioxidant enzyme activities (SOD, CAT and GPx).¹⁹ The antioxidant effect of GLP has become a research hotspot, but the understanding of the antioxidant mechanisms of specific polysaccharides in *G. lucidum* is still limited.

With improved living standards, the fast-paced working and living environment can easily cause a state of oxidative stress in the body.^{20,21} People are paying increasing attention to skin problems caused by oxidation, such as skin aging, inflammation, and even cancer. The human body has its antioxidant enzyme and non-enzyme system (free metals or metal complexes) to resist oxidative damage, including superoxide dismutase (SOD), catalase (CAT), glutathione peroxidase (GSH-Px), and other enzymes that can slow down oxidative damage by scavenging excess-free radicals.²² Sometimes, the oxidative damage caused by excessive reactive oxygen species (ROS) might be too extended for the intrinsic protection system. In this case, lipid peroxidation, DNA damage, and abnormal protein expression will occur. Oxidative stress refers to a state of imbalance between oxidation and antioxidant effects in the body, tending to oxidation, leading to neutrophil inflammatory infiltration, increased protease secretion, and the production of a large number of oxidative intermediates. Oxidative stress is a negative effect caused by free radicals in the body and is considered to be an important factor in aging and disease. In addition, oxidative stress is considered to be the early stage of aging. Most of the health problems associated with aging, such as wrinkles, heart disease and Alzheimer's disease, are linked to excessive oxidative stress in the body.^{23–26} people are increasingly seeking more natural and safer antioxidants and anti-aging drugs. Natural antioxidants are widely used in functional foods, cosmetics, and pharmaceuticals.

Keap1-Nrf2-ARE signaling pathway is one of the most important mechanisms of cellular defense against oxidative stress injury. Transcriptional regulation of many

proteins with detoxification and antioxidant defense functions depends on the activation of Nrf2 signaling pathway. Under oxidative stress, the increase of intracellular Nrf2 may be maintained at a high level by decreasing ubiquitination and Nrf2 degradation.²⁷ When oxidative stress occurs in the body, whether acute or chronic oxidative stress, excessive ROS is produced to cause damage to cell lipids, proteins and DNA, resulting in cell death and tissue damage.²⁸ However, the body also has its own antioxidant mechanism, among which the most extensive is the KEAP1-NRF2-ARE pathway mechanism, which can protect a variety of cells and tissues.²⁹ Yuan et al investigated the protective effect of aloe polysaccharides on skin cells from UVB oxidative damage through Keap1/Nrf2/ARE signaling pathway.³⁰

This study was aimed at screening *G. lucidum* polysaccharides through assessing antioxidant activity in vitro. We established an oxidative damage model by inducing oxidative stress in human skin fibroblasts with H₂O₂, and exploring the protective mechanism of *Ganoderma lucidum* polysaccharides against oxidative damage. It provides the theoretical basis for the development of natural antioxidants.

Materials and Methods

Reagents and Instruments

The following reagents were used following the manufacturers' instructions. The fifth generation of Immortalized Human skin fibroblasts (HSFs) (Cell Resource Centre, Beijing Union Medical College, China); Ascorbic acid (VC), 1-diphenyl-2-picrylhydrazyl (DPPH), ABTS and pyrogallol (Banxia Technologies, China); Fetal bovine serum (FBS), phosphate-buffered solution (PBS), Dulbecco's modified Eagle's medium (DMEM), pancreatin, and 1% antibiotic-antimycotic solution (100 U·mL⁻¹ penicillin/streptomycin and 100 U·mL⁻¹ amphotericin) (Gibco Carlsbad, CA, USA); Dimethyl sulfoxide (DMSO), 3-(4,5-dimethylthiazol-2-yl)-2,5-diphenyltetrazolium bromide (MTT) (Sigma St. Louis, USA); ROS, SOD, CAT, GSH-Px and Malondialdehyde (MDA) assay kits (Beyotime Biotechnologies, Shanghai, China); EasyScript[®] One-Step gDNA Removal and cDNA Synthesis SuperMix and TransStart[®] Top Green qPCR SuperMix (TransGen Biotech Beijing, China). DEAE-52 Anion Exchange Chromatography Column (Beijing Yinglik Technology Development Co., Ltd., China); Olympus Inverted fluorescent microscope (Shanghai Tulsen Vision Technology Co.,

LTD, Shanghai, China); Infinite M200 PRO fluorescence marker (Deken Trading Co., LTD).

Measurement of Antioxidant Activity in vitro

Polysaccharides of 6 different sources of *G. lucidum* (GLP1~6) were prepared according to the method of Zhang et al.³¹ The activated liquid strains of *Ganoderma lucidum* were inoculated in potato culture medium at a volume ratio of 1:10, and cultured in a 180 r/min incubator at 28°C for 7 days. The obtained *Ganoderma lucidum* mycelium was washed twice and lyophilized powder was obtained by freeze-drying. The lyophilized powder was mixed with water at a ratio of 1:30 (m/V) and extracted for 1 h at 70°C to obtain GLP. The six GLPs are different from the *G. lucidum* strains. GLP1 ~ 6 were all purchased from CGMCC of China, with CGMCC numbers 5.896, 5.1817, 5.1816, 5.862, 5.848 and 5.709, respectively.

The DPPH, O²⁻, hydroxyl (·OH), and ABTS-free radical scavenging abilities were measured following previously published methods.³²⁻³⁵ The 759S ultraviolet and visible spectrophotometer was used to determine the absorbance of DPPH at 517 nm, ABTS at 750 nm, HO· at 230 nm, and O^{2*-} at 560 nm.

Cell Culture and MTT Assay

HSFs were maintained in DMEM containing 10% heat-inactivated FBS, and a 1% antibiotic-antimycotic solution consisting of 100 U·mL⁻¹ penicillin/streptomycin, and 100 U·mL⁻¹ amphotericin. Cells were incubated at 37°C in a humidified atmosphere with 5% CO₂. The MTT assay was conducted as in our previously published studies.³⁶ Specifically, discard the old medium, wash the plate with PBS, add MTT solution to the washed PLATE with PBS, add 100μL MTT solution (1g/L) to each well, and put into the cell culture box for incubation for 4h; After discarding MTT solution, 150μL OF DMSO was added to each well, and placed in an incubator for 10min. The OD490 value of each well was measured by an Infinite M200 PRO fluorimeter. Five sub-wells were set in each group, and the average value was taken. Set a blank hole. The blank hole means that no operation is carried out in the culture plate and equal amount of DMSO is added.

Hydrogen Peroxide-Induced Skin Damage Model Establishing

Hydrogen peroxide (H₂O₂) was used to establish the oxidative damage model of HSFs. A wide range of

concentrations of H_2O_2 ($50\sim 1000 \mu\text{mol}\cdot\text{L}^{-1}$) was used to evaluate the effects on the viability changes of HSFs. Cells were seeded in 96-well plates at a density of 1×10^4 cells/well and cultured in DMEM for many hours (1, 2, 3 and 4h). The medium was then discarded, and different concentrations of H_2O_2 solution diluted in FBS-free DMEM were added for the following two hours. Cell viabilities were determined using the colorimetric MTT assay. Morphology changes were observed by Olympus Fluorescence Inverted Microscope (40 \times). Finally, H_2O_2 stimulation at a concentration of $100 \mu\text{mol}\cdot\text{L}^{-1}$ for 2 hours was selected as the modeling condition according to cell viability, and the survival rate was 50%. The number of HSF cells decreased, and the cell morphology changed from normal thin to short round to death and abscission.

When the oxidative damage type was established, the cell survival rate was usually in the range of 50%~70%. If the survival rate is too high, the cells cannot cause obvious oxidative damage; However, if the cell survival rate is too low, it is easy to cause irreversible damage, which is not conducive to the establishment of oxidative damage model.

Experimental Groups

Control group: Cells were seeded in 96-well plates at a density of 1×10^4 cells/well and cultured in DMEM for 24 hours. Then, the medium was discarded, and FBS-free medium was added for the next 24 hours.

Model group in protective study: Cells were seeded in 96-well plates at a density of 1×10^4 cells/well and cultured in DMEM for 24 hours. Then, cells were treated by FBS-free DMEM for 24 hours, followed by $100 \mu\text{mol}\cdot\text{L}^{-1}$ H_2O_2 for 2 hours.

Model group in reparative study: Cells were seeded in 96-well plates at a density of 1×10^4 cells/well and cultured in DMEM for 24 hours. Then, cells were treated by $100 \mu\text{mol}\cdot\text{L}^{-1}$ H_2O_2 for 2 hours, followed by FBS-free DMEM for 24 hours.

Protective group: After culturing for 24 hours, GLP solutions of different concentrations (or the positive control) were added to the culture medium for another 24-hour culturing period, followed by the addition of $100 \mu\text{mol}\cdot\text{L}^{-1}$ H_2O_2 to stimulate the cells for 2 hours.

Reparative group: After culturing for 24 hours, cells were treated with $100 \mu\text{mol}\cdot\text{L}^{-1}$ H_2O_2 for 2 hours, and then GLP solutions of different concentrations (or the

positive control) were added for another 24-hour culturing period.

Purification and Separation of GLPI

Deproteinization was performed following the Sevage method.³⁷ The crude polysaccharides after deproteinization were separated on DEAE-52 ion exchange column. The crude polysaccharide solution of $10 \text{ g}\cdot\text{L}^{-1}$ was added into Sevage's reagent (chloroform: n-butanol = 5:1 (V/V)) at a volume ratio of 1:5. After 30 min of electromagnetic stirring, the solution was transferred to a separating funnel and stood for 10 min to remove the denaturated protein at the junction of the two phases.

Determination of Intracellular MDA, ROS, and SOD, CAT, GSH-Px

The HSF cells were grouped and cultured based on the experimental design. According to the manufacturer's instructions, the supernatant was used to detect MDA content (Beyotime, China). The supernatant's total protein concentrations were determined using the BCA method (Beyotimes, Shanghai, China). The MDA level was quantified and expressed as $\mu\text{mol}\cdot\text{g}^{-1}$ protein. Intracellular ROS levels were detected using a dichloro-dihydro-fluorescein diacetate (DCFH-DA) fluorescent probe (Beyotime, Shanghai, China). DCFH-DA is a general indicator of oxidative stress. Cell membrane permeability, no fluorescence itself. Once in the cell, DCFH is hydrolyzed by cytoesterase to produce DCFH, which is then rapidly oxidized to produce DCF, which can be detected by fluorescence spectroscopy (Ex/Em = 504/529nm). Suitable for the detection of reactive oxygen species (ROS) and nitric oxide (NO), as well as the determination of total oxidative stress levels. It is widely used to monitor cell REDOX processes.

Cell samples were harvested, homogenized, and centrifuged. The total protein concentrations were determined using the BCA kit (Beyotimes, Shanghai, China). Then, the levels of SOD, catalase, and GSH-Px were measured according to the Beyotime assay protocols. The above mentioned three parameters, $\text{U}\cdot\text{mg}^{-1}$, $\text{U}\cdot\text{mg}^{-1}$, and $\text{U}\cdot\text{g}^{-1}$ protein, respectively.

Quantitative Reverse Transcriptional PCR

According to the manufacturer's instructions, total RNAs in different treatment groups were extracted using the RNAprep Pure Cell/Bacteria Kit. Then, cDNA was

synthesized from the RNA using the EasyScript[®] One-Step gDNA Removal and cDNA Synthesis SuperMix, according to the manufacturer's instructions. The cDNA was subjected to PCR amplification using gene-specific primers for Keap1, Nrf2, Nqo1, Ho-1, Gclm, Gclc, Gstm1, Gstt1, and β -actin.

Quantitative real-time PCR (qRT-PCR) was performed using the β -actin gene as an internal control to normalize all RNA expression levels. The subsequent PCR amplification was carried out under the following conditions: the cDNAs were denatured for 2 min at 95°C, followed by PCR (40 cycles of 15 s at 95°C, 20 s at 57°C, and 30 s at 72°C) and a final extension at 95°C for 15 s using Ampli Taq Gold (PerkinElmer).

The Ct (threshold cycle) was calculated at the intersection between an amplification curve and a threshold line. The normalized specific gene expression level was calculated and expressed as follows: $\Delta Ct1 = Ct(\text{target gene treated}) - Ct(\beta\text{-actin treated})$; $\Delta Ct2 = Ct(\text{target gene control}) - Ct(\beta\text{-actin control})$; $\Delta\Delta Ct = \Delta Ct1_{\text{treated}} - \Delta Ct2_{\text{control}}$, and the fold change of the specific gene was $2^{-\Delta\Delta Ct}$.

Statistical Analysis

GraphPad Prism (GraphPad Software, La Jolla, CA) software was used for all statistical analysis. All experiments were performed in triplicate at the minimum. All the data were expressed as mean \pm standard deviation (SD) and analyzed using the Student's *t*-test or one-way ANOVA followed by Turkey's test. Statistical significance was considered to be $p < 0.05$.

Results

Antioxidation of GLP in vitro

Scavenging abilities of DPPH, ABTS, hydroxyl, and superoxide anion free radicals ($O_2^{\cdot-}$) of GLP1-6 in different concentrations are shown in Figure 1. GLP displayed a different antioxidant potential.

GLP quenched DPPH-free radicals in a concentration-dependent manner (Figure 1A). Based on the EC_{50} (50% free radical scavenging concentration, Table 1) value of each GLP, the DPPH scavenging abilities of GLP in a decreasing order were as follows: GLP4 > GLP1 > GLP2 > GLP3 > GLP6 > GLP5. Based on the results obtained, we were unable to calculate the EC_{50} value of GLP5. Therefore, GLP5 is considered to have the poorest capacity in quenching DPPH-free radicals.

The ABTS-free radicals were used to evaluate total antioxidant capacity. GLP1~6 all showed high scavenging abilities. As shown in Figure 1B, GLP1 displayed a relatively high antioxidant potential. GLP1 concentrations ranging from $5\text{g}\cdot\text{L}^{-1}$ to $25\text{g}\cdot\text{L}^{-1}$, showed high antioxidant abilities with the Trolox-equivalent antioxidant capacity ranging from 1.91 to $2.89\text{mmol}\cdot\text{L}^{-1}$.

GLP discussed in the study had different scavenging abilities of hydroxyl radicals (Figure 1C). Among them, GLP1 displayed a relatively high antioxidant potential. At the same concentration ($20\text{g}\cdot\text{L}^{-1}$), GLP1 showed (80.45 ± 0.89) % scavenging ability, while GLP6 showed (19.33 ± 6.00) %. Based on the EC_{50} value (Table 1), the scavenging abilities of hydroxyl radicals of GLPs were as follows: GLP1 > GLP4 > GLP3 > GLP2 > GLP5 and GLP6. EC_{50} values of GLP5 and GLP6 were impossible to be calculated because 50% scavenging value was not obtained within the range of concentrations involved in the study. Each of them quenched hydroxyl radicals in a concentration-dependent manner.

The $O_2^{\cdot-}$ scavenging ability of GLP is shown in Figure 1D. GLP4, and GLP6 increased in a concentration-dependent manner. On the other hand, the abilities of GLP2, GLP3, and GLP5 were around 40%~60%. Based on the EC_{50} (50% free radical scavenging concentration, Table 1) value of each GLP, the $O_2^{\cdot-}$ scavenging abilities of GLP in a decreasing order were as follows: GLP5 > GLP4 > GLP3 > GLP2 > GLP6 > GLP1.

Effects of GLP Pre-Treatments and Post-Treatments on Oxidative Stress HSF Model

The protective and reparative effects of GLP on H_2O_2 -induced damaged HSFs were analyzed and discussed for morphological changes and viabilities. Results are shown in Figure 2. Cells in the control group showed long spindle-shaped radiating cytoplasmic extensions, strong intercellular connection with centrally located nuclei, and were firmly attached to the cell culture dish (Figure 2A1 and A2). However, HSFs in the model group did not have normal morphology (Figure 2B1 and B2). The regular long spindle-shaped radiating shapes were not apparent in the H_2O_2 alone group. The connection between cells was loose, and the distance between cells was broadened. The cell confluence was significantly decreased in the simple H_2O_2 group, and most of the cells were detached from the

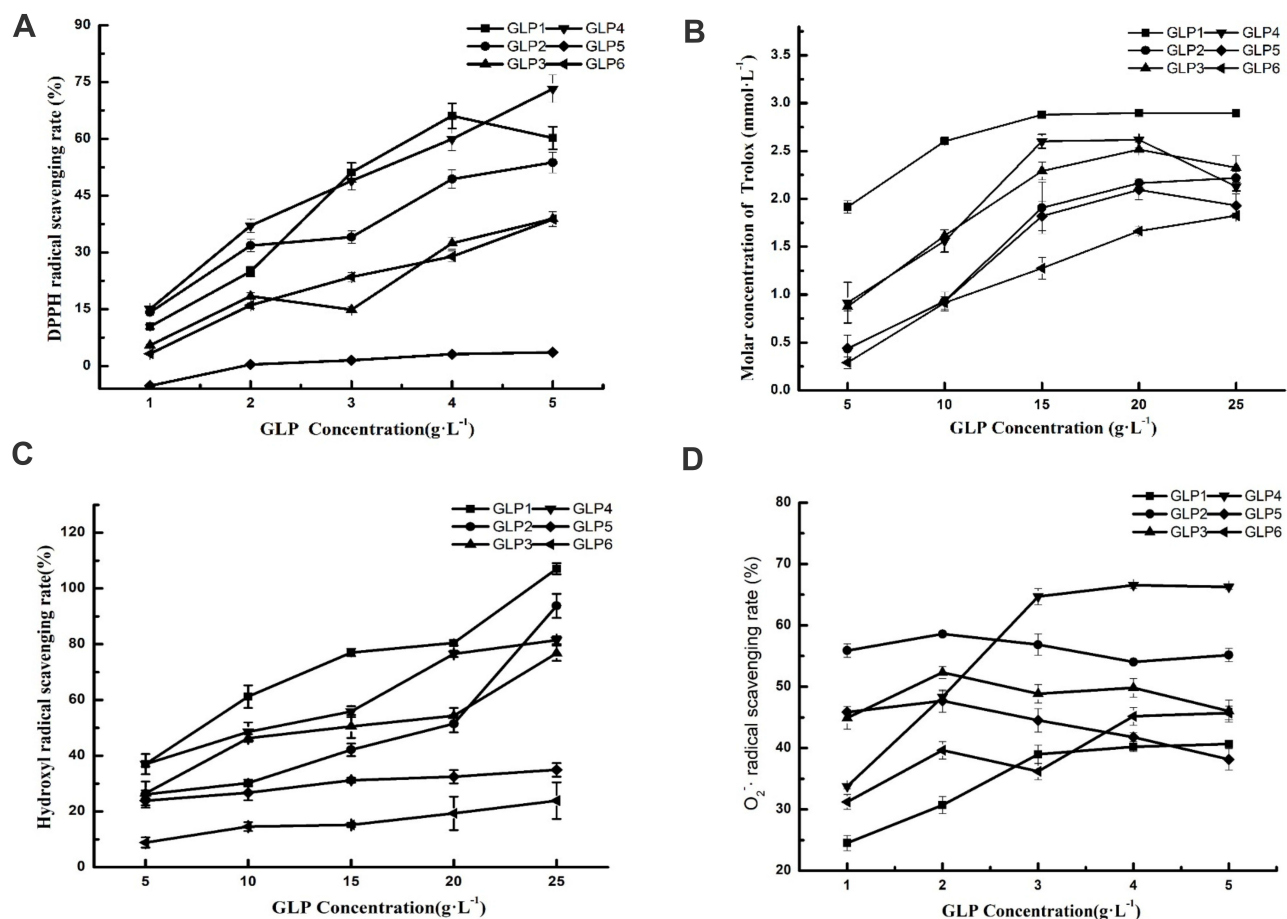


Figure 1 The antioxidant potential of GLPs at different concentrations. Scavenging effects of GLPs on DPPH-free radicals (A), ABTS-free radicals (B), hydroxyl radicals (C), and superoxide anion-free radicals (D). Results are expressed as mean ± SD (n = 3).

culture dish surface and floated in the medium. This cell morphological change was more evident in the repair experimental model group than in the protective experimental model group.

Ascorbic acid (VC) treatment at the concentration of 86 mg·L⁻¹ for 2 hours (IC80) was also chosen as a positive control method. The morphology and the number of cells were improved after the VC treatment in the

protective experiment, compared with the control (Figure 2C1 and J1). HSFs pre-treatment with GLP1~6 followed by 100 μmol·L⁻¹ H₂O₂ for 2 hours and improved cells states (Figure 2D1–I1), compared with the model group. GLP5 group had the highest cell viability, GLP1 group had higher cell viability than the positive control (p < 0.001), and there was no significant difference with GLP5 group (p = 0.5652) (Figure 2J1).

Table 1 EC₅₀ Value of Different Scavenging Abilities

Samples	EC ₅₀ of GLPs (mg/mL)	EC ₅₀ of GLPs (mg/mL)	EC ₅₀ of GLPs (mg/mL)
	DPPH	O ^{2·-}	OH
GLP1	3.15±0.23	9.56±0.71	7.61±0.55
GLP2	4.41±0.51	6.70±0.23	13.34±0.10
GLP3	8.61±0.32	2.78±0.15	12.65±0.85
GLP4	2.85±0.05	2.03±0.11	9.47±0.73
GLP5	–	1.10±0.01	–
GLP6	3.15±0.23	9.56±0.71	7.61±0.55

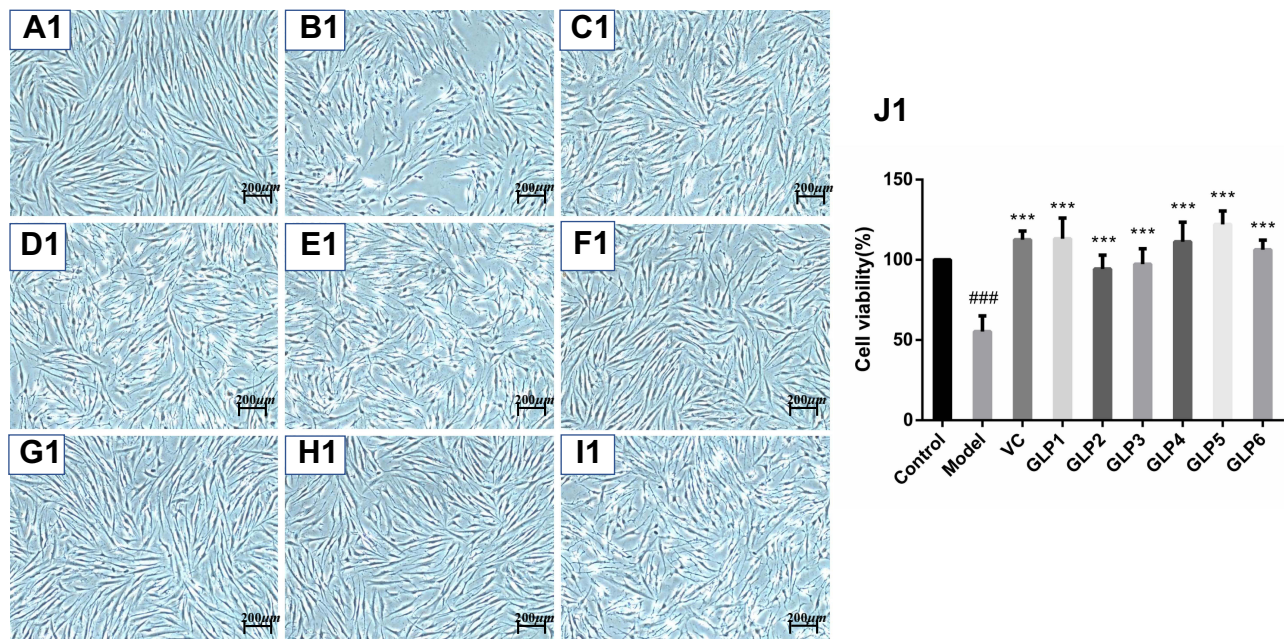


Figure 2 Continue.

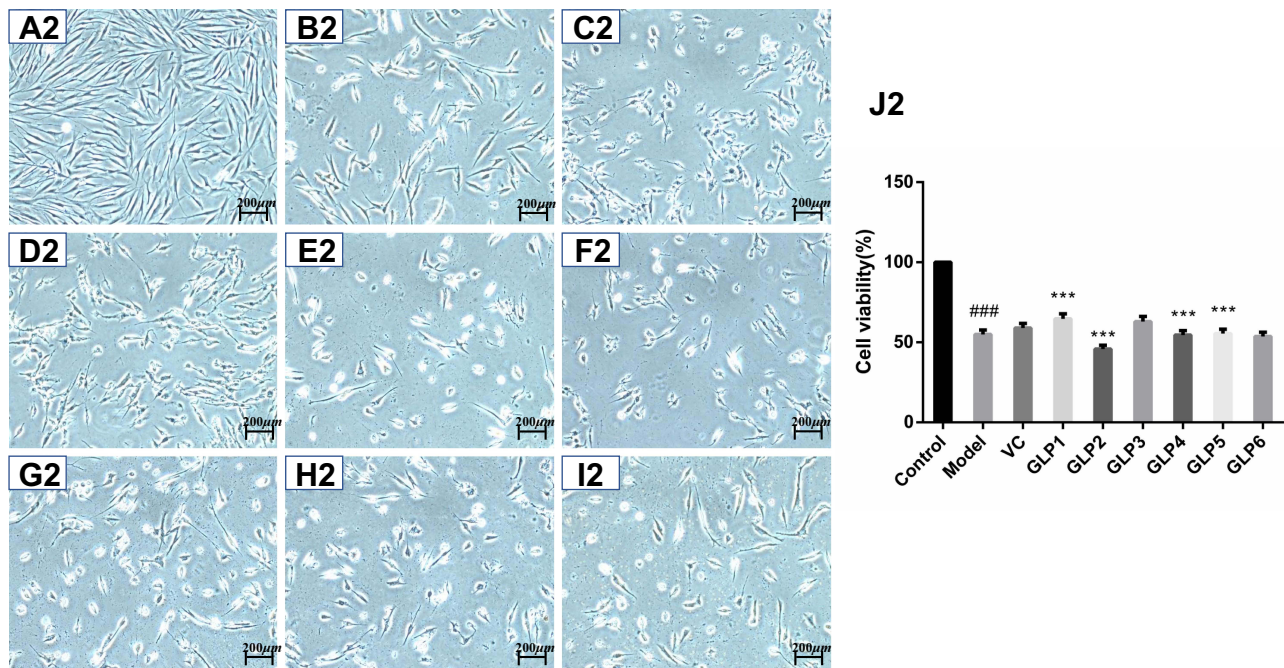


Figure 2 Protective and reparative effects of GLPs treated on H₂O₂-induced oxidative damaged HSFs. **(A1–I1)** shows the protective effects of GLPs. **(A1)** The morphology of HSFs in normal conditions (Control). **(B1)** The morphological changes of cells pretreated with DMEM without FBS for 24h followed by 100 μmol L⁻¹ H₂O₂ for 2 h (model). **(C1)** The morphology of HSFs pretreated with 86 mg L⁻¹ ascorbic acid (VC, considered as a positive control) followed by 100 μmol L⁻¹ H₂O₂ for 2 h. **(D1–I1)** The morphology of HSFs pretreated respectively with GLP1~GLP6 at the concentration of 1.25 g L⁻¹ followed by 100 μmol L⁻¹ H₂O₂ for 2 h. **(J1)** Cell viability was determined using MTT assay. **A2 to J2** shows the reparative effects of GLPs. **(A2)** The morphology of HSFs in normal conditions (Control). **(B2)** The morphological changes of cells pretreated with 100 μmol L⁻¹ H₂O₂ for 2 h followed by DMEM without FBS for 24h (Model). **(C2)** The morphology of HSFs pretreated with 100 μmol L⁻¹ H₂O₂ for 2 h followed by 86 mg L⁻¹ VC. **(D2–I2)** The morphology of HSFs pretreated with 100 μmol L⁻¹ H₂O₂ for 2 h followed by GLP1~GLP6 at the concentration of 1.25 g L⁻¹, respectively. **(J2)** Cell viability was determined using MTT assay. Changes in morphology were observed by Olympus Fluorescence Inverted Microscope (40×). Results are expressed as the mean ± SD (n = 3). The Student's t-test was performed to determine statistical significance (***p < 0.001, versus the control group; ####p < 0.001, versus the model group).

As shown in [Figure 2J2](#), the cell viability after GLP1 repair was the highest and it was significantly higher than that of the model and positive control groups ($p < 0.001$).

In conclusion, combined with the results of GLPs' antioxidant activity in vitro and GLPs' protective and reparative effects on HSFs, GLP1 was selected for further study. In order to find out the proper components that play part in the activity, we performed preliminary purification of GLP1. The deproteinized GLP1 was obtained by Sevage method, and the isolated GLP1I and GLP1II was purified by DEAE-52 ion exchange resin (Elution curve could be seen in [Figure S2](#) in [Supplementary Material](#)). The monosaccharide composition of each component was analyzed by gas chromatography-mass spectrometry (GC-MS, shown in [Figure S3](#) in [Supplementary Material](#)). [Table S1](#) exhibited the standard curves of 10 kinds of monosaccharide. And the results showed that GLP1 and the two components were all composed of three monosaccharides, and glucose had the highest proportion. The other two common monosaccharides are mannose and galactose. Besides, rhamnose and fucose were found in GLP1I, which was considered to be caused by enrichment after purification. Molar ratio of each sample can be found in [Table S2](#) in the [Supplementary Material](#).

Effects of GLP1 on the Levels of Antioxidant Enzymes

[Figure 3A–C](#) shows the activity results of antioxidant enzymes (CAT, GSH-Px and SOD) in cells under the two treatments of protective and reparative. Compared with the model group, the GLP1, GLP1I, GLP1II can significantly improve CAT expression in HSF ($p < 0.001$) in both treatments ([Figure 3A1](#) and [A2](#)). In the protective way, the ability to enhance CAT was as follows: GLP1I > VC > GLP1 > GLP1II ([Figure 3A1](#)). In the reparative way, it was as follows: GLP1I > GLP1II > VC > GLP1 ([Figure 3A2](#)); Compared with model group, GLP1, GLP1I, GLP1II can significantly improve the GSH-Px level of HSFs ($p < 0.001$) in both treatments ([Figure 3B1](#) and [B2](#)). In the protective way, the GSH-Px expression reached $(12.19 \pm 0.61) \text{ U} \cdot \text{g}^{-1}$ after GLP1I treated, higher than the model group by 36.84% ([Figure 3B1](#)). In the reparative way, the GLP1I group of GSH-Px level is 7.56 times that of the model ([Figure 3B2](#)), the GSH-Px levels after three kinds of GLP treated were higher than positive control VC. Compared with the model group, GLP1, GLP1I, and GLP1II can significantly improve the

HSF intracellular SOD activity ($p < 0.001$). Both for protection and repair, SOD activity was higher than in the positive control. Among the different components, GLP1I was the most efficient, compared with the model group. With GLP1I, the expression of SOD was nearly three times higher ([Figure 3C1](#) and [C2](#)).

ROS generation is a common response to cell damage and contributes to apoptotic process.³⁸ In the two ways of protective and reparative, the effects of GLP1 and its components (GLP1I and GLP1II) on ROS production and MDA level results are shown in [Figure 3D](#) and [E](#). Ascorbic acid was used a positive control. ROS and MDA levels were significantly increased ($p < 0.001$) after H_2O_2 stimulation. Compared with the model group, the GLP1, GLP1I, and GLP1II could significantly reduce ROS levels in HSFs. GLP1I was able to remove ROS better than VC. Compared with the model, the GLP1, GLP1I, and GLP1II could significantly reduce the accumulation of MDA in HSF. Regarding the protective effect, the sample's ability to reduce the MDA accumulation was as follows: GLP1II > VC > GLP1 > GLP1I ([Figure 3D1](#)). For the repair function, on the other hand, the sample's ability to reduce the MDA accumulation was: VC > GLP1II > GLP1 > GLP1I ([Figure 3D2](#)). The effects of VC and GLP1II had no significant difference ($P > 0.05$). These results suggest that GLP can protect cells from H_2O_2 oxidative damage by reducing ROS levels ([Figure 3E1](#) and [E2](#)).

Effects of GLP1 on the Expression Alterations of Keap1-Nrf2/ARE Signaling Pathway Markers

The MTT assay showed the noncytotoxic ability of GLPs at concentrations ranging from 0.3125 to $5 \text{ g} \cdot \text{L}^{-1}$ (cell viabilities were all above 80%) (data not shown). Therefore, we selected three concentrations (2.5 , 1.25 , $0.50 \text{ g} \cdot \text{L}^{-1}$) for further study. VC was chosen to be a positive control at the concentration of $86 \text{ mg} \cdot \text{L}^{-1}$ (IC80).

The results of relative gene expressions (Keap1, Nrf2, Gstm1, Gstt1, Gclc, Gclm, Ho-1, and Nqo1) related to Keap1 Nrf2/ARE signaling pathway are shown in [Figure 4](#).

Under the two treated ways, compared with the model group, the GLP1 ($1.25 \text{ g} \cdot \text{L}^{-1}$), GLP1I ($1.25 \text{ g} \cdot \text{L}^{-1}$), and GLP1II ($0.5 \text{ g} \cdot \text{L}^{-1}$) can significantly inhibit the expression of negative regulatory factors Keap1 more than VC. In the repair way, GLP1I showed a dose-dependent

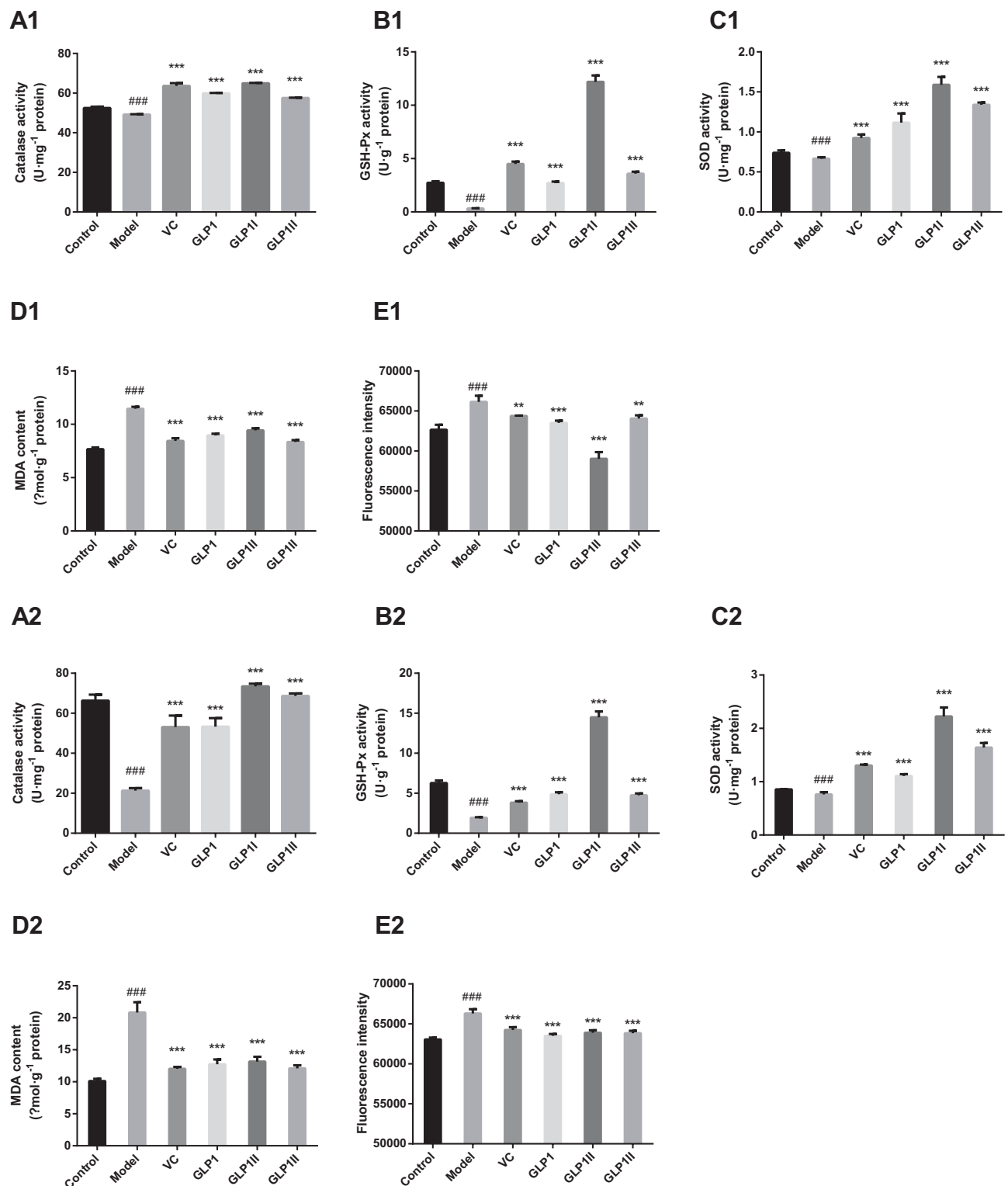


Figure 3 Protective and reparative effects of GLPI, GLPII, and GLPIII treated on H₂O₂-induced oxidative damaged HSFs. VC was considered as a positive control. (A1–E1) shows the protective effects of GLPI, GLPII, and GLPIII. HSFs were pretreated respectively with GLPI, GLPII, and GLPIII at the concentration of 1.25 g L⁻¹ followed by 100 μmol L⁻¹ H₂O₂ for 2 h. (A2–E2) shows the reparative effects of GLPI, GLPII, and GLPIII. HSFs were pretreated with 100 μmol L⁻¹ H₂O₂ for 2 h, followed by GLPI, GLPII, and GLPIII at the concentration of 1.25 g L⁻¹, respectively. (A1 and A2) catalase activities; (B1 and B2), GSH-Px activities; (C1 and C2) SOD activities; (D1 and D2) MDA contents; (E1 and E2) ROS levels represented by fluorescence intensity. Results are expressed as the mean ± SD (n = 3). The Student's t-test was performed to determine statistical significance (**P < 0.01, ***P < 0.001, versus the control group; ####P < 0.001, versus the model group).

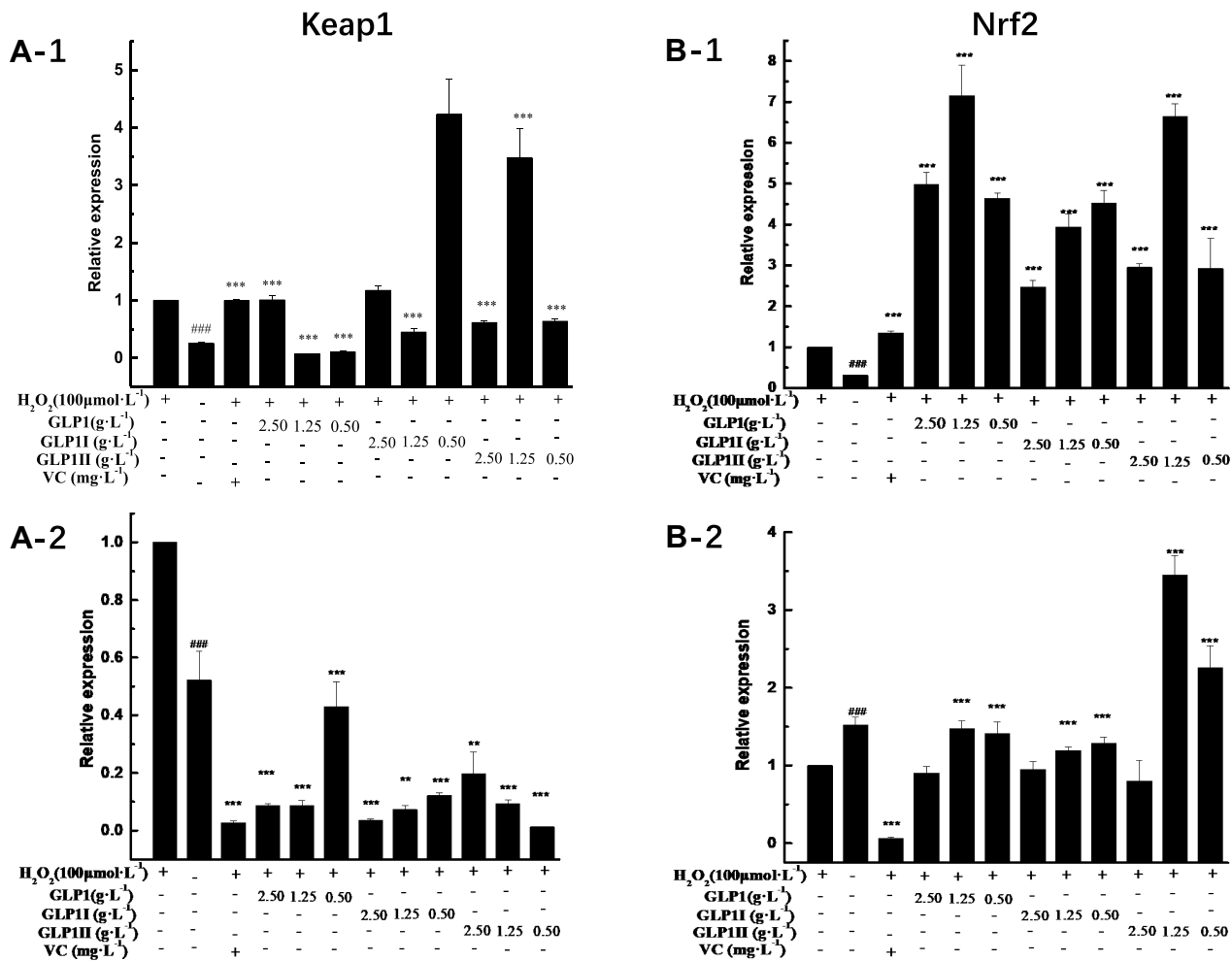


Figure 4 Continue.

(Figure 4A1 and A2) ($p < 0.001$); The GLP1 (1.25 $\text{g}\cdot\text{L}^{-1}$), GLP1I (0.5 $\text{g}\cdot\text{L}^{-1}$) and GLP1II (1.25 $\text{g}\cdot\text{L}^{-1}$) could significantly activate the expression of key regulatory factors Nrf2 (Figure 4B1 and B2). Glutathione S transferase (GSTs) is the body's most important II metabolic enzymes. GSTs to ROS and MDA activation of electrophilic reagents give play to the role of detoxification. In the protect way, only GLP1 (2.5 $\text{g}\cdot\text{L}^{-1}$) significantly enhanced the expression of Gstm1 (Figure 4C1) ($p < 0.001$), but all sample groups significantly increased the expression of Gstt1 (Figure 3D1). In the repair way, GLP1 (1.25, 0.5 $\text{g}\cdot\text{L}^{-1}$), GLP1I (1.25, 0.5 $\text{g}\cdot\text{L}^{-1}$) and GLP1II (2.5, 1.25 $\text{g}\cdot\text{L}^{-1}$) could significantly increase the expression of Gstm1 and Gstt1 (Figure 4C2 and D2); Glutamate cysteine ligase (Gcl) is a critical enzyme in the synthesis of GSH, and its catalytic subunit (Gclc) and regulatory subunit (Gclm) play crucial roles in

enhancing the ability of anti-oxidative stress. Under the two treated ways, a high concentration of GLP1, GLP1I and GLP1II (2.5, 1.25 $\text{g}\cdot\text{L}^{-1}$) can significantly increase the expression of Gclc (Figure 4E1 and E2). In the protect way, the expression of Gclm was significantly enhanced by GLP1 and GLP1II. However, GLP1I promotes Gclm expression in a dose-dependent manner, as long as the high concentration showed a boost (Figure 4F1). In the repair way, GLP1 could significantly increase the expression of Gclm (Figure 4F2). Heme oxygenase-1 (Ho-1) plays an important role in eliminating ROS and protecting against peroxides, peroxynitrites, hydroxyl groups, and superoxide free radicals. GLP1, GLP1I, and GLP1II significantly promoted the expression of Ho-1 (Figure 4G1 and G2). GLP1 (2.5 $\text{g}\cdot\text{L}^{-1}$) and GLP1II (1.25 $\text{g}\cdot\text{L}^{-1}$) could significantly increase the expression of Nqo1 (Figure 4H1 and H2) ($p < 0.001$).

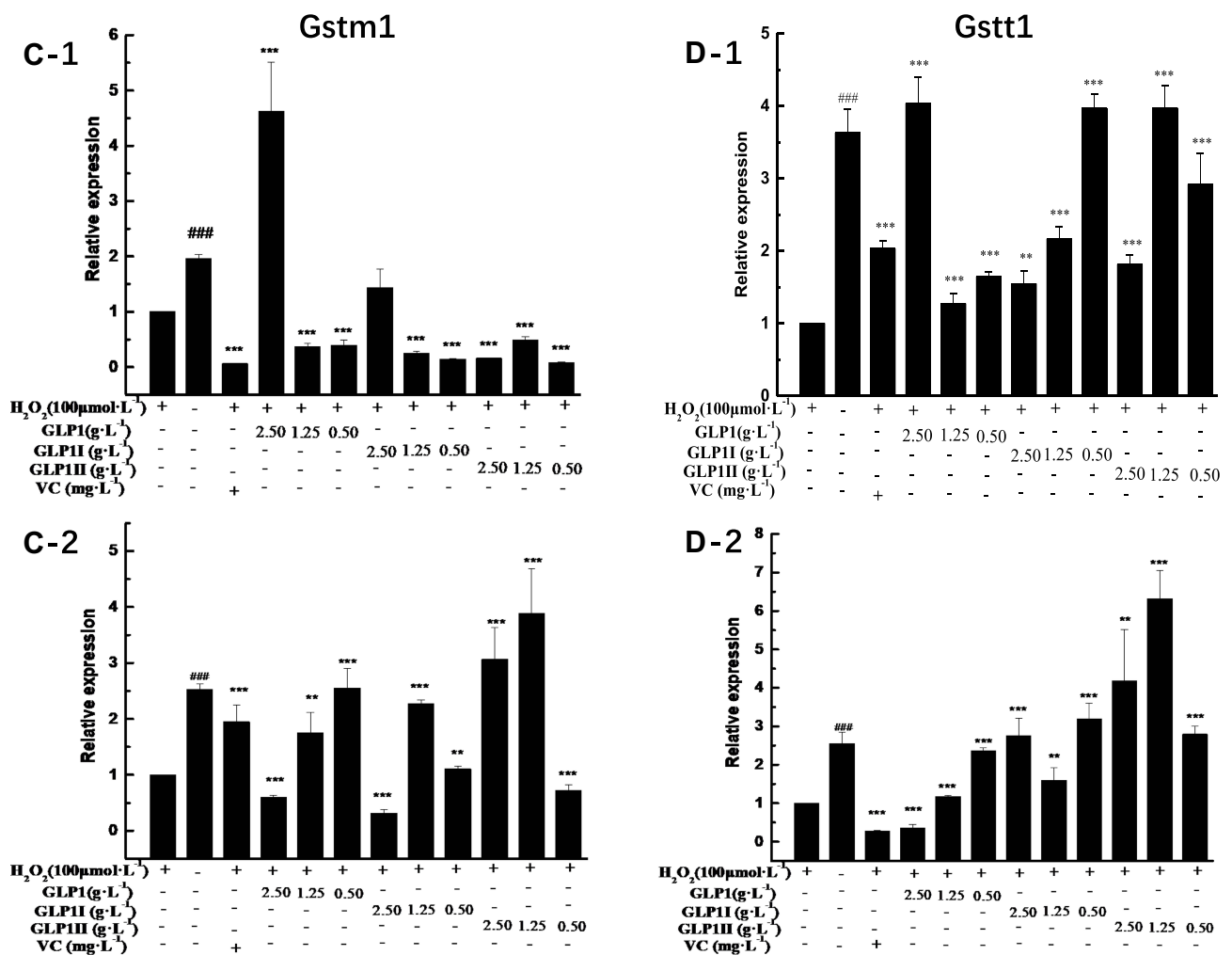


Figure 4 Continue.

Discussion

GLP is one of the main active ingredients of *Ganoderma lucidum*. A large number of studies have shown that it has high development value in the aspect of antioxidants. Li et al suggested the GLP may serve as an effective strategy for fatty liver treatment.¹⁵ There have been reported GLP is a potent antioxidant against the pathogenesis of atherosclerosis instable angina in high-risk patients.³⁹ GLP can also exert hypolipidemic, antioxidant, and antiapoptotic effects in HD-induced obese mice.¹⁸ However, GLP has a wide variety and molecular weight distribution. In this study, a total of 6 GLPs were extracted to study their antioxidant activity in vitro and their protective and reparative effects on oxidation-damaged HSFs. The results showed that GLP1 had an outstanding ability to scavenge ABTS-free radicals, hydroxyl-free radicals, and DPPH-free radicals and had great protective and reparative effects

on oxidative damage of HSF. In addition, GLP1 showed the most significant improvement in cell viability under the two treatments. Interestingly, in our study, we found a difference in cell morphology between the two treatments. Compared with normal cells, morphological changes were more obvious in the repair experimental model group than in the protection experimental model group. The reason for this may be the different order in which the culture medium and the hydrogen peroxide were added. After being treated with DMEM for 24 hours, the cells were more tolerant to the cell damage caused by H₂O₂. However, after H₂O₂ damaged the cells, the morphology changed, and oxidative stress occurred. When the cells were further cultured in the FBS-free DMEM environment, the cells' repair system could not resist the external starvation environment, resulting in more severe cell oxidative damage. Finally, GLP1 was selected as the

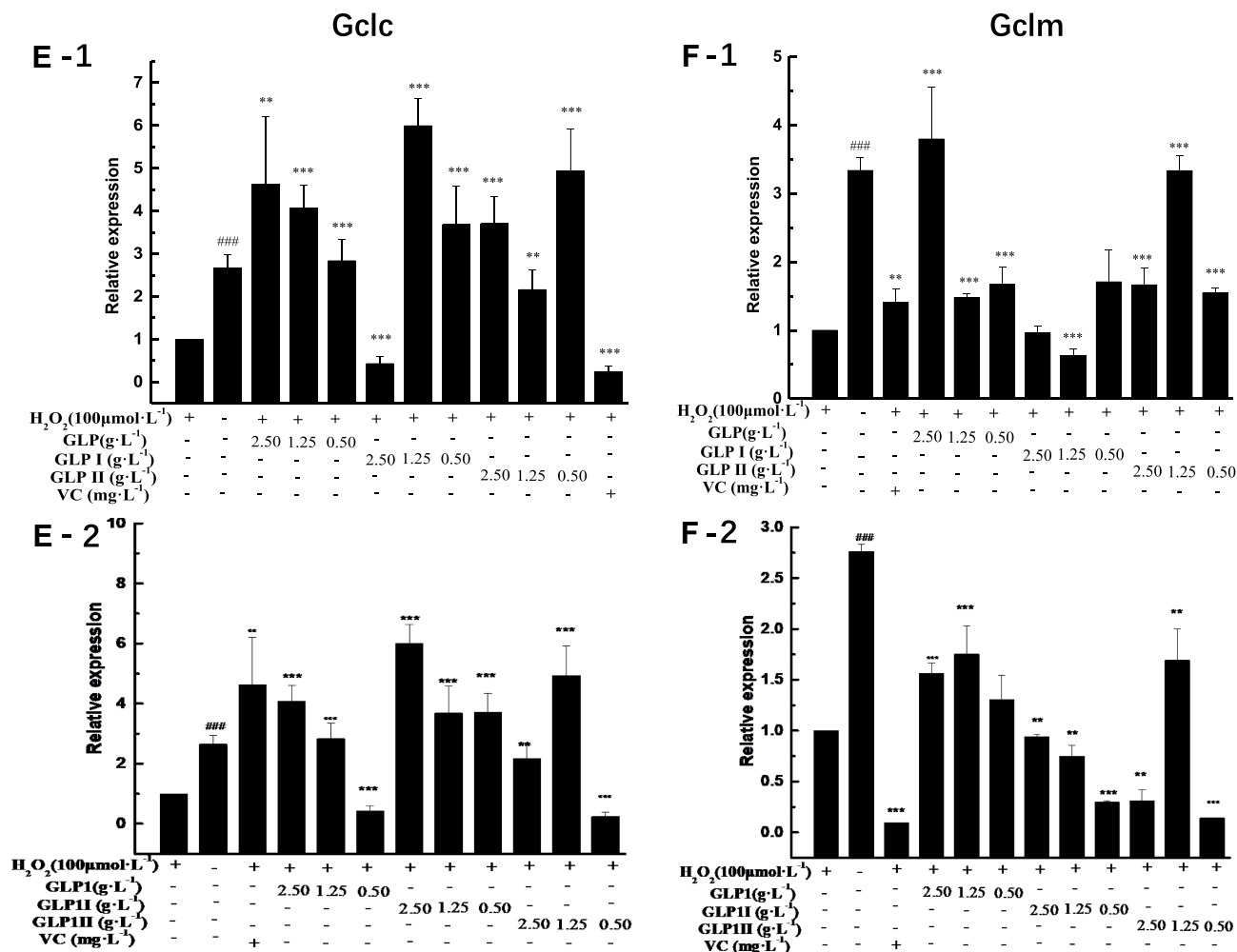


Figure 4 Continue.

optimal polysaccharide. We separated GLP1 and obtained two components, namely GLP1I and GLP1II. By comparing the GC spectra of the two components, we found that both polysaccharides contained mannose, galactose and glucose, but rhamnose and fucose were found in GLP1I, which we thought might be caused by enrichment after purification. Previous studies have isolated polysaccharide structures containing galactose, rhamnose and glucose from the structure characterization of *G. lucidum* fruit body polysaccharides.⁴⁰ Another study also isolated two components of GLP, and the antioxidant results showed that both had antioxidant activity.⁴¹ In the future, the two polysaccharide components can be systematically characterized and physicochemical analysis, comparative analysis of their structural differences, and then discuss their efficacy.

When oxidative stress occurs, excessive accumulation of ROS can lead to dysregulation of the body's antioxidant

system.⁴² The oxidation product MDA destroys cell membrane integrity, affects cell structure, changes ion transport, and leads to dysfunction of cell energy metabolism. The content of MDA can reflect the level of lipid peroxidation and the damage degree of cell lipid peroxidation to some extent.⁴³ Antioxidant enzymes SOD, CAT, and GSH-Px are the primary substances for scavenging free radicals in organisms, and their levels in organisms indicate an intuitive index of oxidative damage rate.⁴⁴ Most studies have shown that antioxidants are an important step in preventing aging because the build-up of ROS can lead to DNA damage, which has been shown to have a significant impact on aging.^{45,46} In the past, the role of DNA damage response in aging has been described.⁴⁷ The results of this study indicate that GLP1 and its components can significantly reduce ROS and MDA contents in the oxidative damage model. In addition, whether in reparative or protective, GLP1, GLP1I, GLP1II can significantly

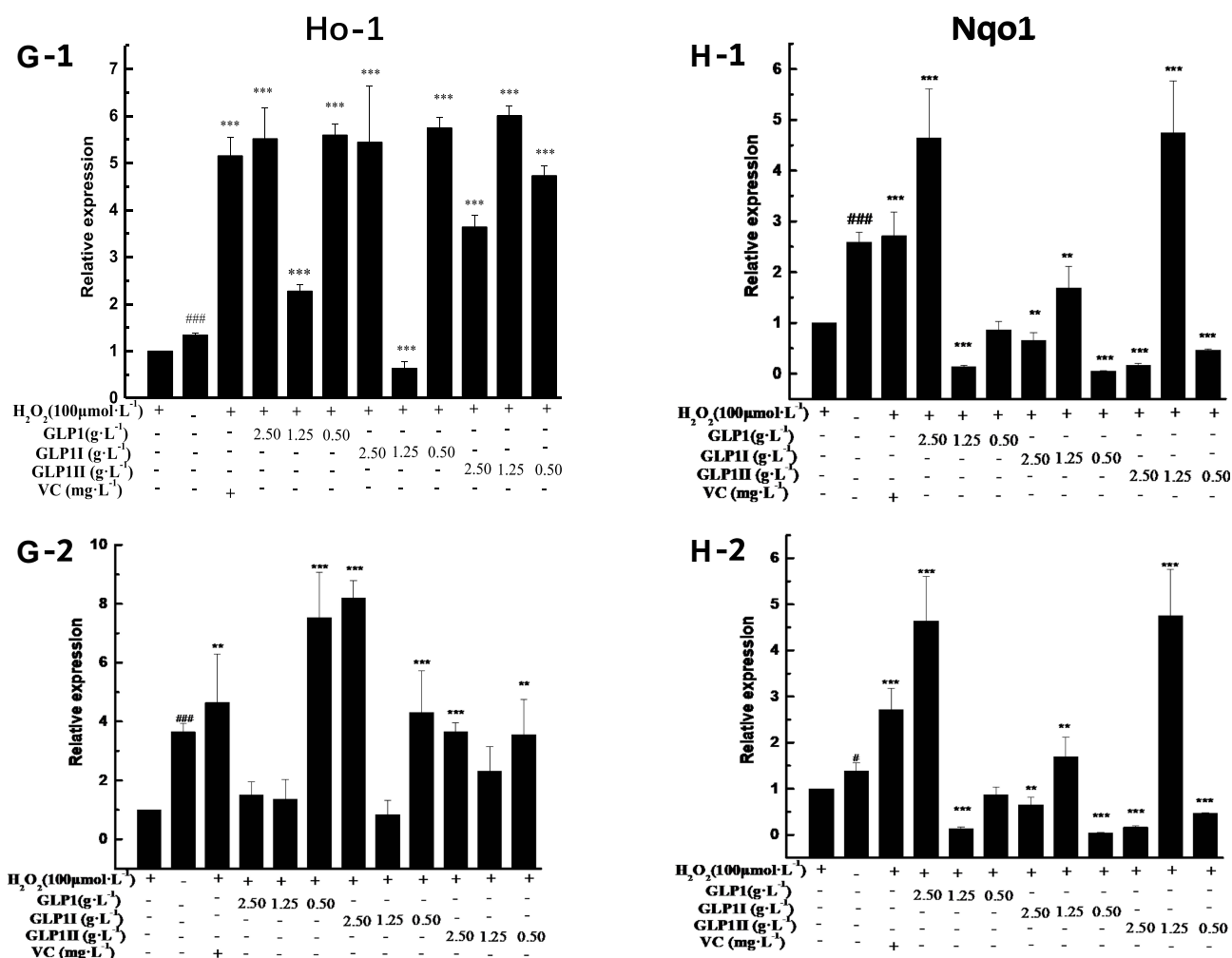


Figure 4 Effects of GLP1, GLP1I, and GLP1II on the expressions of genes related to Keap1/Nrf2-ARE signaling pathway. **(A1 and A2)** Keap1; **(B1 and B2)** Nrf2; **(C1 and C2)** Gstm1; **(D1 and D2)** Gstm1; **(E1 and E2)** Gclm; **(F1 and F2)** Gclm; **(G1 and G2)** Ho-1; **(H1 and H2)** Nqo1. A1 to H1 shows the protective effects of GLP1, GLP1I, and GLP1II. HSFs were pretreated respectively with GLP1, GLP1I, and GLP1II at the concentration of 0.5, 1.25, and 2.5 g·L⁻¹ followed by 100 μmol·L⁻¹ H₂O₂ for 2 h. **(A2–E2)** shows the reparative effects of GLP1, GLP1I, and GLP1II. HSFs were pretreated with 100 μmol·L⁻¹ H₂O₂ for 2 h, followed by GLP1, GLP1I, and GLP1II at the concentration of 0.5, 1.25 and 2.5 g·L⁻¹, respectively. Results are expressed as the mean ± SD (n = 3). The Student's t-test was performed to determine statistical significance (**P < 0.01, ***P < 0.001, versus the control group; ###P < 0.001, versus the model group).

improve three kinds of antioxidant enzymes (SOD, CAT, and GSH-Px) expression, GLP1I had the most significant effect. This indicates that GLP1 and its components can scavenge free radicals by reducing oxidation products and increasing the expression of antioxidant enzymes, thus protecting HSF from oxidative damage caused by H₂O₂, which in turn acts as an anti-aging agent. This is consistent with previous review reports on the potential mechanism of *Ganoderma lucidum*'s anti-aging effect and its clinical application.¹¹ In addition, there have been reports showing that degraded polysaccharides from *G. lucidum* have stronger hypolipidemic and antioxidant activities than natural polysaccharides from *Ganoderma lucidum*.⁴⁸

Keap1/Nrf2-mediated signaling pathway is an essential signaling pathway for maintaining oxidative stress and redox

balance in the body.⁴⁹ Nrf2 is a key transcription factor that regulates redox balance. Under normal physiological conditions, Keap1 and Nrf2 combine to form a complex, and Nrf2 is degraded continuously, which keeps the Nrf2 content in the body at a low level.⁵⁰ When the body is under oxidative stress, the conformational change of cysteine residue of Keap1 makes the bound Nrf2 disintegrate and enter the nucleus to bind to ARE, regulate the expression of downstream antioxidant proteins and detoxifying enzymes, and transcribe Ho-1 and Nqo1, reducing the effect of oxidative stress on cells and tissues.^{51,52} Previous studies have reported that Keap1-Nrf2/ARE signaling acts as a key pathway for the cellular antioxidant activity of fisetin.⁵³ The protective effect of sulforaphane on cadmium-induced oxidative damage of mouse stromal cells has been studied through the Nrf2/ARE

signaling pathway.⁵⁴ Therefore, we studied the mechanism of antioxidant damage of GLP through the Keap1-Nrf2/ARE signaling pathway. As one of the active oxygen species, H₂O₂ is not only easy to pass through the cell membrane and react with intracellular iron ions to generate highly active free radicals but also easy to obtain and stable in nature, and has become an important tool for studying various kinds of cell oxidative damage at home and abroad.^{55,56} The gene expression of antioxidant enzymes is mediated by antioxidant response elements (ARE), and nuclear factor-related factor-2 (Nrf2) can up-regulate the gene expression of ARE-mediated antioxidant enzymes. The results showed that GLP1 and its components can significantly increase the levels of SOD, CAT and GSH-Px. Meanwhile, Nrf2, a key regulator of Keap1-NRF2 /ARE signaling pathway, was activated, while Keap1, a negative regulator, was inhibited, thus promoting the expression of downstream antioxidant enzyme genes (GSTs, GCLs, Nqo1, and Ho-1). Therefore, GLP1 and its components protected HSFs from oxidative damage of H₂O₂ by activating the Keap1-Nrf2/ARE signaling pathway.

Conclusion

Through the determination of antioxidant activity and cell viability in vitro, we screened the optimal polysaccharide GLP1 from six GLPs, separating the two components from GLP11 (GLPII, GLPIII). The study found that GLP1 and its components can reduce ROS and MDA content, increase the antioxidant enzymes SOD, CAT, and GSH-Px of expression, and through the activation of Keap1-Nrf2/ARE signaling pathway to protect HSFs from oxidative damage induced by H₂O₂. GLP has the potential to be used as a natural antioxidant in cosmetics and health products. This study provides a theoretical basis and data support for the development of anti-aging cosmetics based on natural plant materials. In future studies, complete characterization and structure analysis of the two polysaccharide components can be carried out.

Acknowledgments

Upon the completion of this manuscript, we would like to express our heartfelt thanks to Beijing Technology and Business University for providing us with an excellent learning platform, a rich scientific research environment, a warm campus environment, and an excellent and responsible and kind teacher. We would also like to thank the editors and review experts who will carefully review our manuscript and suggest reasonable modifications; In addition, I also want to thank my parents and

friends for the care in my study and life! Finally, I would like to express my heartfelt thanks to all the friends who have helped me.

Disclosure

The authors report no conflicts of interest in this work.

References

- Zhao C, Zhang C, Xing Z, Ahmad Z, Li JS, Chang MW. Pharmacological effects of natural Ganoderma and its extracts on neurological diseases: a comprehensive review. *Int J Biol Macromol*. 2019;121:1160–1178. doi:10.1016/j.ijbiomac.2018.10.076
- Ji Z, Tang Q, Zhang J, Yang Y, Jia W, Pan Y. Immunomodulation of RAW264.7 macrophages by GLIS, a proteopolysaccharide from *Ganoderma lucidum*. *J Ethnopharmacol*. 2007;112(3):445–450. doi:10.1016/j.jep.2007.03.035
- Ren L, Zhang J, Zhang T. Immunomodulatory activities of polysaccharides from *Ganoderma* on immune effector cells. *Food Chem*. 2021;340:127933. doi:10.1016/j.foodchem.2020.127933
- Wang SY, Hsu ML, Hsu HC, et al. The anti-tumor effect of *Ganoderma lucidum* is mediated by cytokines released from activated macrophages and T lymphocytes. *Int J Cancer*. 1997;70(6):699–705. doi:10.1002/(SICI)1097-0215(19970317)70:6<699::AID-IJC12>3.0.CO;2-5
- Petrova ES, Rudina MI, Shvarts YS. Antitumor potential of substances from the fungus *Ganoderma lucidum*. *Pharm Chem J*. 2018;52(1):57–62. doi:10.1007/s11094-018-1765-x
- Li L, Xu JX, Cao YJ, et al. Preparation of *Ganoderma lucidum* polysaccharide chromium (III) complex and its hypoglycemic and hypolipidemic activities in high-fat and high-fructose diet-induced pre-diabetic mice. *Int J Biol Macromol*. 2019;140:782–793. doi:10.1016/j.ijbiomac.2019.08.072
- Santesso N, Wieland LS. A summary of a Cochrane Review: ganoderma lucidum (Reishi mushroom) for the treatment of cancer. *Eur J Integr Med*. 2016;8(5):619–620. doi:10.1016/j.eujim.2016.07.025
- Raseta M, Popovic M, Beara I, et al. Anti-inflammatory, antioxidant and enzyme inhibition activities in correlation with mycochemical profile of selected indigenous *Ganoderma* spp. from Balkan region (Serbia). *Chem Biodivers*. 2020;18(2):e2000828.
- Krobthong S, Yingchutrakul Y. Identification and enhancement of antioxidant P1-peptide isolated from *Ganoderma lucidum* hydrolysate. *Food Biotechnol*. 2020;34(4):338–351. doi:10.1080/08905436.2020.1844228
- Hu Z, Du R, Xiu L, et al. Protective effect of triterpenes of *Ganoderma lucidum* on lipopolysaccharide-induced inflammatory responses and acute liver injury. *Cytokine*. 2020;127:154917. doi:10.1016/j.cyto.2019.154917
- Wang J, Cao B, Zhao H, Feng J. Emerging roles of ganoderma lucidum in anti-aging. *Aging Dis*. 2017;8(6):691–707. doi:10.14336/AD.2017.0410
- Huie CW, Di X. Chromatographic and electrophoretic methods for Lingzhi pharmacologically active components. *J Chromatogr B Analyt Technol Biomed Life Sci*. 2004;812(1–2):241–257. doi:10.1016/S1570-0232(04)00678-6
- Cor D, Knez Z, Knez Hrcic M. Antitumor, antimicrobial, antioxidant and antiacetylcholinesterase effect of *Ganoderma lucidum* Terpenoids and Polysaccharides: a review. *Molecules*. 2018;23(3):647. doi:10.3390/molecules23030649
- Lu J, He R, Sun P, Zhang F, Linhardt RJ, Zhang A. Molecular mechanisms of bioactive polysaccharides from *Ganoderma lucidum* (Lingzhi), a review. *Int J Biol Macromol*. 2020;150:765–774. doi:10.1016/j.ijbiomac.2020.02.035

15. Li HN, Zhao LL, Zhou DY, Chen DQ. Ganoderma lucidum polysaccharides ameliorates hepatic steatosis and oxidative stress in db/db mice via targeting nuclear factor E2 (Erythroid-Derived 2)-related factor-2/heme oxygenase-1 (HO-1) pathway. *Med Sci Monit.* 2020;26:e921905.
16. Zheng S, Zhang W, Liu S. Optimization of ultrasonic-assisted extraction of polysaccharides and triterpenoids from the medicinal mushroom Ganoderma lucidum and evaluation of their in vitro antioxidant capacities. *PLoS One.* 2020;15(12):e0244749. doi:10.1371/journal.pone.0244749
17. Zeng X, Li P, Chen X, et al. Effects of deproteinization methods on primary structure and antioxidant activity of Ganoderma lucidum polysaccharides. *Int J Biol Macromol.* 2019;126:867–876. doi:10.1016/j.ijbiomac.2018.12.222
18. Liang Z, Yuan Z, Li G, Fu F, Shan Y. Hypolipidemic, antioxidant, and antiapoptotic effects of polysaccharides extracted from Reishi Mushroom, Ganoderma lucidum (Leysser: Fr) Karst, in mice fed a high-fat diet. *J Med Food.* 2018;21(12):1218–1227. doi:10.1089/jmf.2018.4182
19. Chen XP, Chen Y, Li SP, Chen YG, Lan JY, Liu LP. Free radical scavenging of Ganoderma lucidum polysaccharides and its effect on antioxidant enzymes and immunity activities in cervical carcinoma rats. *Carbohydr Polym.* 2009;77(2):389–393. doi:10.1016/j.carbpol.2009.01.009
20. Wei Y, Omaye ST. Air pollutants, oxidative stress and human health. *Mutat Res.* 2009;674(1–2):45–54. doi:10.1016/j.mrgentox.2008.10.005
21. Finkel T, Holbrook NJ. Oxidants, oxidative stress and the biology of ageing. *Nature.* 2000;408(6809):239–247. doi:10.1038/35041687
22. Getoff N. Anti-aging and aging factors in life. The role of free radicals. *Radiat Phys Chem.* 2007;76(10):1577–1586. doi:10.1016/j.radphyschem.2007.01.002
23. Lephart ED. Skin aging and oxidative stress: equol's anti-aging effects via biochemical and molecular mechanisms. *Ageing Res Rev.* 2016;31:36–54. doi:10.1016/j.arr.2016.08.001
24. Poprac P, Jomova K, Simunkova M, Kollar V, Rhodes CJ, Valko M. Targeting free radicals in oxidative stress-related human diseases. *Trends Pharmacol Sci.* 2017;38(7):592–607. doi:10.1016/j.tips.2017.04.005
25. Reczek CR, Chandel NS. ROS-dependent signal transduction. *Curr Opin Cell Biol.* 2015;33:8–13. doi:10.1016/j.ceb.2014.09.010
26. Lara J, Sherratt MJ, Rees M. Aging and anti-aging. *Maturitas.* 2016;93:1–3. doi:10.1016/j.maturitas.2016.08.020
27. Hu R, Saw CL, Yu R, Kong AN. Regulation of Nrf2 Signaling for cancer chemoprevention: antioxidant coupled with anti-inflammatory. *Antioxid Redox Signal.* 2010;13(11):1679–1698. doi:10.1089/ars.2010.3276
28. Halliwell B. Antioxidants in human health and disease. *Annu Rev Nutr.* 1996;16(1):33–50. doi:10.1146/annurev.nu.16.070196.000341
29. Ramos-Gomez M, Kwak MK, Dolan PM, et al. Sensitivity to carcinogenesis is increased and chemoprotective efficacy of enzyme inducers is lost in Nrf2 transcription factor-deficient mice. *Proc Natl Acad Sci USA.* 2001;98(6):3410–3415.
30. Yuan LL, Duan XW, Zhang RT, Zhang YB, Qu MW. Aloe polysaccharide protects skin cells from UVB irradiation through Keap1/Nrf2/ARE signal pathway. *J Dermatol Treat.* 2019;31(3):1–27.
31. Zhang JC, Shao Q, Wang Q, et al. Protective mechanism of polysaccharides from Ganoderma lucidum mycelium against oxidative stress injury of human skin fibroblasts. *Food Sci.* 2020;41(13):174–183.
32. Zhang M, Zhang H, Li H, et al. Antioxidant mechanism of betaine without free radical scavenging ability. *J Agric Food Chem.* 2016;64(42):7921–7930. doi:10.1021/acs.jafc.6b03592
33. Zi Y, Zhang B, Jiang B, et al. Antioxidant action and protective and reparative effects of lentinan on oxidative damage in HaCaT cells. *J Cosmet Dermatol.* 2018;17(6):1108–1114. doi:10.1111/jocd.12488
34. Smirnoff N, Cumbes QJ. Hydroxyl radical scavenging activity of compatible solutes. *Phytochemistry.* 1989;28(4):1057–1060. doi:10.1016/0031-9422(89)80182-7
35. Li XC, Lin J, Gao YX, Han WJ, Chen DF. Antioxidant activity and mechanism of Rhizoma cisticifugae. *Chem Cent J.* 2012;6(1):1–10.
36. You SQ, Shi XQ, Yu D, et al. Fermentation of Panax notoginseng root extract polysaccharides attenuates oxidative stress and promotes type I procollagen synthesis in human dermal fibroblast cells. *BMC Complement Med Ther.* 2021;21(1):1
37. Liu LQ. Study on extraction, purification, structure characterization and quality control of ganoderma lucidum tea. Guizhou Normal University; 2017.
38. Liu TF, Han YW, Zhou T, Zhang RH, Chen H, Zhao HY. Mechanisms of ROS-induced mitochondria-dependent apoptosis underlying liquid storage of goat spermatozoa. *Ageing.* 2019;11(18):7880–7898.
39. Sargowo D, Ovianti N, Susilowati E, et al. The role of polysaccharide peptide of Ganoderma lucidum as a potent antioxidant against atherosclerosis in high risk and stable angina patients. *Indian Heart J.* 2018;70(5):608–614. doi:10.1016/j.ihj.2017.12.007
40. Pan D, Wang LQ, Chen CH, et al. Structure characterization of a novel neutral polysaccharide isolated from Ganoderma lucidum fruiting bodies. *Food Chem.* 2012;135(3):1097–1103. doi:10.1016/j.foodchem.2012.05.071
41. Liu W, Wang H, Pang X, Yao WG. Characterization and antioxidant activity of two low-molecular-weight polysaccharides purified from the fruiting bodies of Ganoderma lucidum. *Int J Biol Macromol.* 2010;46(4):451–457. doi:10.1016/j.ijbiomac.2010.02.006
42. Yang L, Tan GY, Fu YQ, Feng JH, Zhang MH. Effects of acute heat stress and subsequent stress removal on function of hepatic mitochondrial respiration, ROS production and lipid peroxidation in broiler chickens. *Comp Biochem Physiol C Toxicol Pharmacol.* 2010;151(2):204–208. doi:10.1016/j.cbpc.2009.10.010
43. Jove M, Mota-Martorell N, Pradas I, Martin-Gari M, Ayala V, Pamplona R. The advanced lipoxidation end-product malondialdehyde-lysine in aging and longevity. *Antioxidants.* 2020;9(11):1132. doi:10.3390/antiox9111132
44. Bhatti JS, Bhatti GK, Reddy PH. Mitochondrial dysfunction and oxidative stress in metabolic disorders - A step towards mitochondria based therapeutic strategies. *Biochim Biophys Acta Mol Basis Dis.* 2017;1863(5):1066–1077. doi:10.1016/j.bbdis.2016.11.010
45. Zhao Z, Dong QY, Liu XH, et al. Dynamic transcriptome profiling in DNA damage-induced cellular senescence and transient cell-cycle arrest. *Genomics.* 2020;112(2):1309–1317. doi:10.1016/j.ygeno.2019.07.020
46. Luceri C, Bigagli E, Femia AP, Caderni G, Giovannelli L, Lodovici M. Aging related changes in circulating reactive oxygen species (ROS) and protein carbonyls are indicative of liver oxidative injury. *Toxicol Rep.* 2018;5:141–145. doi:10.1016/j.toxrep.2017.12.017
47. Ling OH, Björn S. DNA damage responses and p53 in the aging process. *Blood.* 2018;131(5):488–495. doi:10.1182/blood-2017-07-746396
48. Xu Y, Zhang X, Yan XH, et al. Characterization, hypolipidemic and antioxidant activities of degraded polysaccharides from Ganoderma lucidum. *Int J Biol Macromol.* 2019;135:706–716. doi:10.1016/j.ijbiomac.2019.05.166
49. Stepkowski TM, Kruszewski MK. Molecular cross-talk between the NRF2/KEAP1 signaling pathway, autophagy, and apoptosis. *Free Radic Biol Med.* 2011;50(9):1186–1195. doi:10.1016/j.freeradbiomed.2011.01.033
50. Suzuki T, Yamamoto M. Stress-sensing mechanisms and the physiological roles of the Keap1-Nrf2 system during cellular stress. *J Biol Chem.* 2017;292(41):16817–16824. doi:10.1074/jbc.R117.800169
51. Canning P, Sorrell FJ, Bullock AN. Structural basis of Keap1 interactions with Nrf2. *Free Radic Biol Med.* 2015;88:101–107. doi:10.1016/j.freeradbiomed.2015.05.034

52. Suzuki T, Yamamoto M. Molecular basis of the Keap1-Nrf2 system. *Free Radic Biol Med.* 2015;88:93–100. doi:10.1016/j.freeradbiomed.2015.06.006
53. Zhang H, Zheng W, Feng X, et al. Nrf2(-)ARE signaling acts as master pathway for the cellular antioxidant activity of Fisetin. *Molecules.* 2019;24(4):708.
54. Yang SH, Li P, Yu LH, et al. Sulforaphane protect against cadmium-induced oxidative damage in mouse Leydigs cells by activating Nrf2/ARE signaling pathway. *Int J Mol Sci.* 2019;20(3):630.
55. Chen T, Guo ZP, Jiao XY, Zhang JY, Liu HJ. Protective effects of peoniflorin against hydrogen peroxide-induced oxidative stress in human umbilical vein endothelial cells. *Can J Physiol Pharmacol.* 2011;89(6):445–453. doi:10.1139/y11-034
56. Park KJ, Kim YJ, Kim J, et al. Protective effects of peroxiredoxin on hydrogen peroxide induced oxidative stress and apoptosis in cardiomyocytes. *Korean Circ J.* 2012;42(1):23–32. doi:10.4070/kcj.2012.42.1.23

Clinical, Cosmetic and Investigational Dermatology

Dovepress

Publish your work in this journal

Clinical, Cosmetic and Investigational Dermatology is an international, peer-reviewed, open access, online journal that focuses on the latest clinical and experimental research in all aspects of skin disease and cosmetic interventions. This journal is indexed on CAS.

The manuscript management system is completely online and includes a very quick and fair peer-review system, which is all easy to use. Visit <http://www.dovepress.com/testimonials.php> to read real quotes from published authors.

Submit your manuscript here: <https://www.dovepress.com/clinical-cosmetic-and-investigational-dermatology-journal>